

Variations of Complex Permittivity due to Water Content and Heavy Metal Contamination

함수비와 중금속 오염도에 따른 유전상수의 변화

Oh, Myoung-Hak¹

오 명 학

Kim, Yong-Sung²

김 용 성

Yoo, Dong-Ju³

유 동 주

Park, Jun-Boum⁴

박 준 범

요 지

지반오염조사에 대한 유전상수 측정기법의 적용성을 평가하기 위하여 함수비와 중금속 오염도에 따른 흙의 유전특성 변화를 분석하였다. 유전상수의 실수부와 허수부 모두 체적함수비에 따른 증가경향을 나타내었으며, 특히 MHz 범위에서 유전상수 실수부는 쌍극자모멘트에 비례하기 때문에 흙의 유전상수는 체적함수비에 따른 선형적인 증가경향을 나타내었다. 중금속 용액은 50 kHz 이하의 저주파영역에서 전극분극효과에 의해 농도 증가에 따라 유전상수 실수부가 증가하였으나, 고주파 영역에서는 이온의 수화작용에 의한 물분자의 배향분극 발현의 감소로 인하여 감소하는 경향을 나타내었다. 유전상수 허수부는 중금속 농도 증가에 따라 전도손실의 증가에 의하여 모든 주파수 영역에서 증가하는 경향을 나타내었다. 흙과 중금속 혼합시료의 경우 함수비가 큰 시료에서는 중금속 용액 자체의 유전특성이 그대로 발현되었으나, 함수비가 작은 시료에서는 공간전하분극의 영향이 우세하여 유전상수 실수부가 10-20%정도 증가하는 경향을 나타내었다. 유전상수 허수부의 경우에는 중금속 농도 증가에 따른 뚜렷한 증가경향을 확인할 수 있었다. 본 연구의 결과에 의하면 중금속의 오염감지에 대해서는 유전상수 실수부보다는 허수부의 적용성이 높은 것으로 나타났으며, 현장에서의 정확한 오염도 평가를 위해서는 함수비에 대한 평가가 선행되어야 할 것으로 판단된다.

Abstract

Laboratory experiments were performed to examine the effects of water content and to see if permittivity had sufficient sensitivity to identify subsurface contamination. Both real and imaginary permittivities of unsaturated sand were strongly governed by the volumetric water content. Especially, a linear relationship between real permittivity and volumetric water content was derived at high frequencies (MHz ranges). Heavy metals in pore fluid result in significant increases in the effective imaginary permittivity, due to ionic conduction, but decreases in the real permittivity arises due to the decreased orientational polarization of water molecules caused by hydration of ions. Clear increase in the effective imaginary permittivity with heavy metal concentration was found to be valuable in the application of electrical methods for detecting heavy metals in the subsurface. However, because the permittivity is primarily dependent on the volumetric water content of soil, pre-evaluation on the volumetric water content is required.

Keywords : Heavy metal, Permittivity, Subsurface contamination, Volumetric water content

1 Member, Post-doc., Research Institute of Energy and Resources, Seoul National Univ., omyhak2@snu.ac.kr

2 Member, Graduate Student, School of Civil, Urban & Geosystem Engrg., Seoul National Univ.

3 Member, Graduate Student, School of Civil, Urban & Geosystem Engrg., Seoul National Univ.

4 Member, Associate Prof., School of Civil, Urban & Geosystem Engrg., Seoul National Univ.

1. Introduction

Detecting and monitoring subsurface contamination are essential processes for preventing potential environmental risks. In conventional approaches, representative samples of soil and pore fluid are collected in the field and analyzed for contaminants in the laboratory. However, such conventional method has the following shortcomings: (1) soil sampling is extremely time consuming and expensive; (2) samples can be contaminated during collection, transportation and analysis in the laboratory (Okoye et al. 1995; Kaya and Fang 1997); and (3) samples require expensive laboratory analyses (Wilson et al. 1995). With regard to the disadvantages mentioned above, a lot of studies have tried to develop an in-situ, simple and cost-effective detecting method. In-situ monitoring using an electrical method has been proposed as a potential alternative by many researcher (Kaya and Fang 1997; Rowe et al. 2001; Fukue et al. 2001; Lindsay et al. 2002). This method is based on the concept that the electrical properties reflect the physical and chemical properties of subsurface materials, with contamination of the subsurface being likely to change the electrical properties. Detection or monitoring by measuring the electrical properties is advantageous, as this is fast, with little data processing required to obtain accurate and repeatable results (Rinaldi and Cuestas 2002).

There are two electrical properties that can be applied in the estimation of subsurface contamination: the electrical resistivity and permittivity. When electric field is applied to a medium, charges act in two different ways within the material. Some charges readily move in a material medium, creating a current of free charges. The electrical conductivity or resistivity of the medium characterizes this property. Other charges are bound, yet these positive and negative charges can move locally relative to each other in the presence of an electric field, resulting in a polarized medium. This polarizability is represented by the permittivity of a medium.

The permittivity of soils has been studied by several researchers in the last decades. The main goal of most of these studies were directed to identifying the variables

that control the permittivity of soil (Thevanayagam 1995; Gardner et al. 1998). Recently, some researchers have proposed potential availability of permittivity in estimating subsurface contamination through laboratory experiments (Kaya and Fang 1997; Santamarina and Fam 1997; Darayan et al. 1998; Rowe et al. 2002; Francisca and Rinaldi 2003). Although heavy metals are the most common contaminants in the subsurface, few data are available on their electrical properties.

In this study, complex permittivity of soils was measured at the frequency range of 1 kHz to 12 MHz. Laboratory experiments were performed to examine the effects of water content and heavy metal contamination on the permittivity of soil. From the test results, the measured electrical properties were evaluated to see if they had sufficient sensitivity to identify subsurface contamination.

2. Experimental Setup for Measuring Permittivity

2.1 Test Materials

Two kinds of soil including Jumunjin sand and a local soil were used in this study. The local soil was collected from Seoul National University and will herefrom be termed as 'SNU soil' for clarifying sample designation. SNU soil is weathered granite soil which is commonly found around the Korean peninsula. Jumunjin sand was classified as poorly graded sand (SP) and SNU soil was classified as well-graded sand (SW). The soils were air dried, sieved through sieve No. 10, and then oven dried at 105°C over 24 hours. Soil-water mixture was put into an acrylic mold and directly compacted to the designed dry density. Both gravimetric water content and total unit weight of soil samples were evaluated. Laboratory experiments were performed for the remolded soil samples with various gravimetric water content and unit weight.

Mercury (Hg), lead (Pb) and cadmium (Cd) were used in this study as representative cationic heavy metals due to their importance as environmental contaminants. Besides heavy metals, aluminum (Al) with different valence and atomic weight was included as a cationic species for

Table 1. Index properties of heavy metals and Aluminum used in this study

	Mercury (Hg)	Lead (Pb)	Cadmium (Cd)	Aluminum (Al)
Atomic number ¹⁾	80	82	48	13
Atomic weight ¹⁾	200.59	207.2	112.41	26.98
Ionic valence ¹⁾	+1	+2	+2	+3
Atomic radius ¹⁾ [Å]	1.50	1.75	1.49	1.43
Ionic radius ¹⁾ [Å]	1.27	1.20	0.97	0.51
Ionic mobility ²⁾ [m ² /Vs]	2.8×10^{-8}	3.7×10^{-8}	3.3×10^{-8}	6.5×10^{-8}

¹⁾ source : Oxtoby and Nachtrieb (1996)

²⁾ source : Dean (1999) and Vanysek (2002).

comparison. The index properties of cationic species used in this study are summarized in Table 1.

2.2 Permittivity Measurement

The two-electrode cell is commonly used to measure the electrical properties of material under the AC electric field. A measuring cell was designed for this study as shown in Figure 1 (a). The two brass electrodes of capacitor-type cell are 70 mm in diameter and are 20 mm apart. Sample was placed between the two electrodes of the acrylic mold for measurement. Such a method enabled an adequate control and preservation of the physical properties of soils during preparation and measurement.

In this study, measurements were performed at frequency ranges between 100 Hz and 10 MHz. Low frequency measurements turn into an advantage in the

following aspects: (1) in-situ testing and monitoring can be performed with little influence of cable impedance; (2) low frequency test devices enable comparatively less expensive measurement; and (3) laboratory tests can be performed with very simple capacitive cells (Rinaldi and Redolfi 1996). The measurements were achieved using the HP4285A Precision LCR meter in the range of 75 kHz to 10 MHz and the Agilent 4263B LCR meter in the range of 100 Hz to 100 kHz. Figure 2 shows the capacitor-type cell and LCR meter used in this study. Both devices allow measurement of capacitance and resistance of an unknown material under test. Electrodes of cell are connected to a bridge-type measuring system by employing Kelvin clip leads (Agilent 16089A) for connection to the cell from the LCR meter. Both electrodes act as current and potential terminals: high current H_c, high potential H_p, low current L_c, and low potential L_p connectors. The configuration of connection

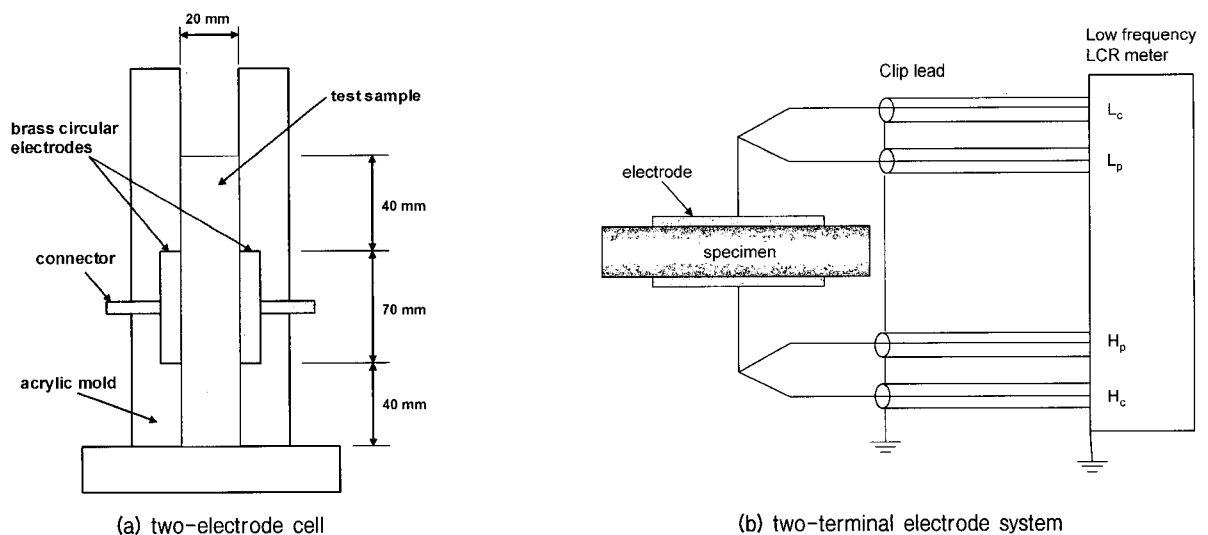
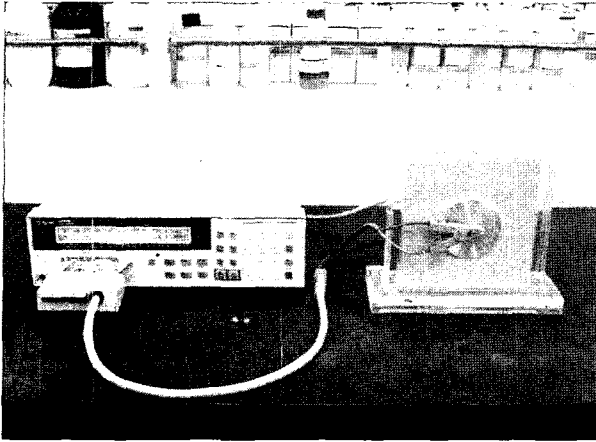
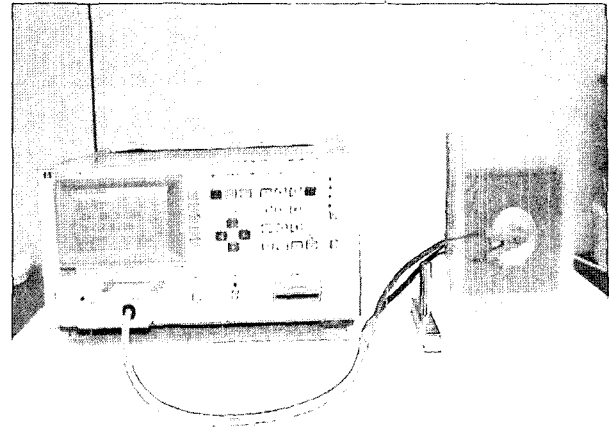


Fig. 1. Schematic diagrams of permittivity measurements



(a) Agilent 4263B LCR meter



(b) HP4285A Precision LCR meter

Fig. 2. Capacitor-type cell connected to LCR meter

of the shields is shown in Figure 1 (b). A sinusoidal excitation is imposed and measurements were repeated at different frequencies.

In permittivity measurement, there are unwanted residual parameters in series and in parallel with the specimen being tested. To remove the influence of residual parameters of wire and clip leads, calibrations were performed by standard short and open circuit calibration procedures. In addition to the residual parameters, edge capacitance which develops at the fringe of the specimen must be compensated. Due to the formation of undesirable flow of electric current, the measured capacitance is larger than the actual capacitance of the material. This effect is further magnified when the ratio between the thickness and diameter of the test specimen increases. In this study, the edge capacitance was removed using the following equation given from ASTM D150 (1994):

$$C_e = (0.0019\kappa' - 0.00252\ln d + 0.0068)p_e \quad (1)$$

$$p_e = \pi(r + d) \quad (2)$$

where, C_e is the edge capacitance [pF], p_e is the modified perimeter of the electrode plate [mm], r is the radius of circular electrode and d is the thickness of specimen. Therefore, capacitance of the specimen can be calculated by subtracting the edge capacitance from the measured capacitance (C_m). The real and effective imaginary permittivities were obtained from the following equations (Agilent Technology 2000):

$$\kappa' = \frac{C_m - C_e}{C_0} = \frac{C_m - C_e}{\epsilon_0 \times \frac{A}{d}} \quad (3)$$

$$\kappa'' = \frac{1}{\omega \epsilon_0 R \times \frac{A}{d}} \quad (4)$$

where, R is the measured resistance, A is the area of the electrodes, d is the distance between electrodes, and ω is the angular frequency ($=2\pi f$).

The permittivity obtained from the capacitor-type cell was finally calibrated with air, carbon tetrachloride (CCl_4), methanol and deionized water at all measuring frequencies. The real permittivity of each selected material at 20°C is constant of 1, 2.17, 31 and 79, respectively, in the frequency range used in this study (von Hippel 1954). Measurements were duplicated and then each of two measured values for capacitance and resistance was averaged, only when their deviation lied within a range of 5%. However, the measured values at 100 Hz were omitted in the analysis since the measuring device showed a tendency of displaying erratic capacitance values at this frequency.

3. Results and Discussion

3.1 Effect of Water Content on Permittivity

The permittivity is governed by volumetric water content, defined as the ratio of the volume of pore water to the total volume of soil, since permittivity is proportional to

the number of dipole moments per unit volume (Oh et al. 2005). The volumetric water content (θ_v) is the ratio of the volume of pore water (V_w) to the total volume of soil (V_t) and is related to the gravimetric water content (w) and the dry unit weight of soil (γ_d) as represented in the following equation:

$$\theta_v = \frac{V_w}{V_t} = \frac{\gamma_d w}{\gamma_w} \quad (5)$$

where, γ_w is the unit weight of water.

There are empirical relationships and mixture models that relate water content to real permittivity based on experiments performed above MHz ranges. Mixture formulas for modeling experimental results are summarized in Table 2. Lundien (1971) presented an empirical formulation between real permittivity and moisture density, defined as the volume of water per unit volume of soil. Here, if unit weight of water is equal to 1 g/cm³, moisture density has the same value as volumetric water content. In addition, Topp et al. (1980) reported an empirical formula for various soils at frequencies between 1 MHz and 1 GHz known as Topp's equation.

The real permittivity of heterogeneous materials is governed by the permittivity of individual components. The resultant permittivity of the mixture measured at the frequency ranged from 100 MHz to 1 GHz can be evaluated through expressions known as mixture models. The three-phase mixture model can be used to indicate how soil components contribute to the real permittivity of bulk soil. For three-phase mixture of air, solid and water, one of the most useful and simple empirical models can be written as follows (Gardner et al. 1998; Robinson et al. 1999).

$$(\kappa')^\alpha = f_a(\kappa'_a)^\alpha + f_s(\kappa'_s)^\alpha + f_w(\kappa'_w)^\alpha \quad (6)$$

$$f_a + f_s + f_w = 1 \quad (7)$$

where, κ'_a , κ'_s , and κ'_w are the real permittivity of air, soil particle and water, respectively, f_a , f_s and f_w are their volume fractions and exponent α can take any value between 0 and 1.

The volume fractions of soil components can be expressed in terms of porosity (n) and volumetric water content. Therefore, equation (6) can be rewritten as equation (8).

$$(\kappa')^\alpha = (n - \theta_v)(\kappa'_a)^\alpha + (1 - n)(\kappa'_s)^\alpha + \theta_v(\kappa'_w)^\alpha \quad (8)$$

If exponent α is set equal to 1/3, the expression becomes identical to the Looyenga model. Especially, with an index of 0.5, the equation is known as CRIM (Complex Refractive Index Method) (Gardner et al. 1998; Robinson et al. 1999; Francisca and Rinaldi 2003). The CRIM and the Looyenga models are most commonly accepted in literature. Similarly, the logarithmic model is a volumetric mixture formula with respect to the logarithms of the permittivities of phase components.

Various empirical relationships between real permittivity and volumetric water content in literature imply that volumetric water content is an effective parameter for describing the permittivity of soil. It is noted that these relationships were derived at frequencies above MHz range.

Figure 3 illustrates the experimental data for the Jumunjin sand and the SNU soil obtained at 10 MHz in this study and the calculated real permittivities from different mixture models and empirical equations. In the calculation of real permittivity using mixture models, measured values for dry soil, tap water and air at 10 MHz were substituted as the real permittivity of each

Table 2. Mixture formulas for modeling the experimental results

	Equation	Frequency	Variables
Lundien equation	$m_d = \frac{\kappa'}{80} - \frac{0.26}{\kappa' - 1} + 0.11$	unspecified frequency	m_d : moisture density
Topp's equation	$\kappa' = 3.03 + 9.3\theta_v + 146.0\theta_v^2 - 76.7\theta_v^3$	1 MHz - 1 GHz	n : porosity θ_v : volumetric water content
CRIM model	$\sqrt{\kappa'} = (n - \theta_v)\sqrt{\kappa'_a} + (1 - n)\sqrt{\kappa'_s} + \theta_v\sqrt{\kappa'_w}$	100 MHz - 1 GHz	κ' : the permittivity of soil mass κ'_a , κ'_s , and κ'_w : the permittivity of air, soil particle and water
Looyenga model	$(\kappa')^{1/3} = (n - \theta_v)(\kappa'_a)^{1/3} + (1 - n)(\kappa'_s)^{1/3} + \theta_v(\kappa'_w)^{1/3}$		
Logarithmic model	$\log(\kappa') = (n - \theta_v)\log(\kappa'_a) + (1 - n)\log(\kappa'_s) + \theta_v\log(\kappa'_w)$		

component for calculation. It can be seen that the real permittivity of test soil was linearly related to the volumetric water content. This result indicates that the volumetric water content could be the most effective indicator for describing the real permittivity of a given soil. However, as shown in Figure 3, the real permittivity calculated by mixture model and empirical formulas was underestimated, especially for the SNU soil, since they did not consider the presence of spatial polarization. The spatial polarization was found to be the main mechanism for two or three phase mixture soils selected in this study. Although spatial polarization tends to manifest at lower frequencies below MHz ranges and is not considered to be significant at frequencies above a few MHz ranges, it is believed that the real permittivity can still be affected by spatial polarization at frequencies up to 10 MHz. Therefore, the effect of spatial polarization on real permittivity of soil should not be totally neglected even at MHz frequencies. However, the relationship between soil properties and real permittivity based on a quantitative analysis on spatial polarization has yet been suggested in literature. In order to apply the mixture model for real permittivity over a wide range of frequencies, modifications to the existing mixture models should be suggested taking into account the development of spatial polarization.

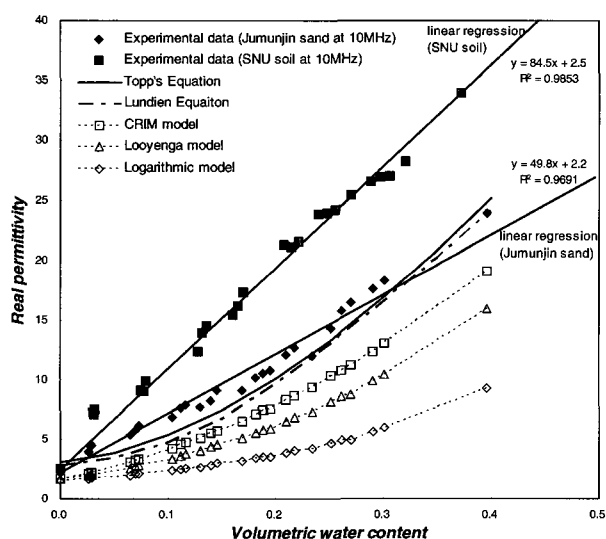


Fig. 3. Comparison of experimental data for the real permittivity of Jumunjin sand and SNU soil obtained at 10 MHz and various empirical relations reported in literature

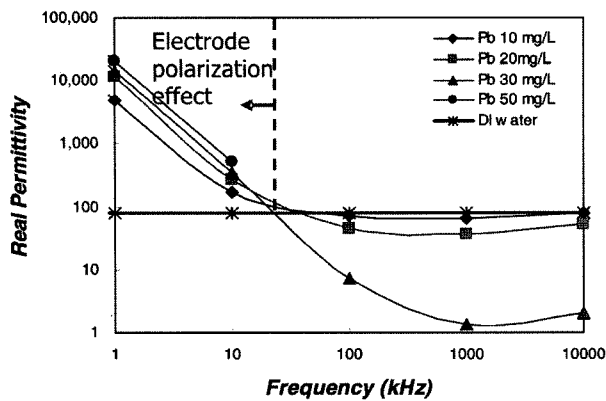
3.2 Effect of Heavy Metal Contamination on Permittivity

3.2.1 Permittivity of Heavy Metal Solutions

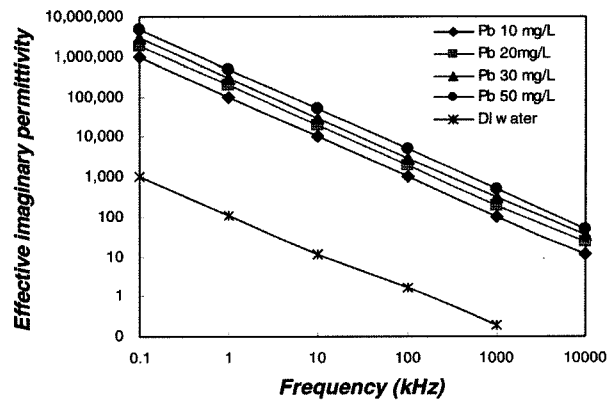
The effect of heavy metal concentration of solutions on the complex permittivity was explored. The spectral responses of complex permittivity of lead at frequency ranges from 1 kHz to 10 MHz are shown in Figure 4.

Figure 4 (a) shows results from two-terminal electrode measurements for deionized water and lead (Pb) solutions. Significant increase in real permittivity values was observed at lower frequencies below 50 kHz. Such an increase in real permittivity was caused by electrode polarization which results from the charge accumulation at the electrode-specimen interface. The minimum frequency at which electrode polarization does not significantly affect the real permittivity measurements is known as the limiting lower frequency. The limiting lower frequency is proportional to the ionic conductivity of the material, therefore highly conductive specimens are affected by electrode polarization to a higher degree than less conductive materials. The range where electrode polarization effects are suspected is denoted on the real permittivity data as shown in Figure 4 (a). Therefore, analysis on permittivity should be performed at frequencies above 50 kHz in order to exclude electrode polarization effect since the increase in real permittivity due to electrode polarization effect is not representative of material properties (Santamarina 2001).

However, above 50 kHz, the decrease in real permittivity with concentration was observed in Figure 4 (a). Such decreases reflect the reduced mobility of water molecules involved in ion hydration. Heavy metal ions dissolved in water affect the molecular interaction between water and ionic species. Water molecules may be firmly bonded to the ions and behave like electrolyte molecules. The hydration of ions renders hydrated ions, which are surrounded by water molecules with hindered polarizability. Water involved with hydrating ions in electrolytes makes a lower contribution to global polarization than free water, resulting in a lower real permittivity of electrolyte solutions at higher concentrations (Santamarina 2001).



(a) real permittivity



(b) effective imaginary permittivity

Fig. 4. Spectral responses for complex permittivity of lead solution

The effective imaginary permittivity increases with an increase in heavy metal concentration. The effective imaginary permittivity data capture conduction loss and/or polarization loss. The increase in effective imaginary permittivity for cationic species solutions with increasing concentration is primarily due to higher conduction losses since electric conduction is enhanced by free movement of cationic species that act as charge carriers.

3.2.2 Permittivity of Soil-heavy Metal Mixtures

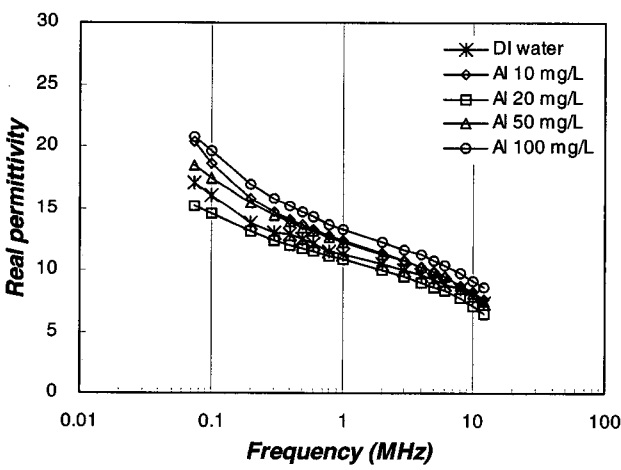
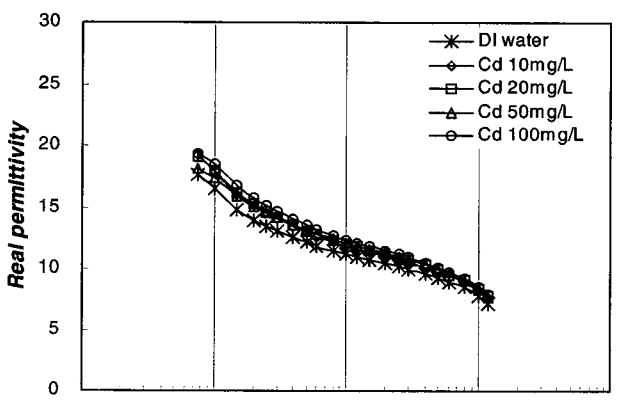
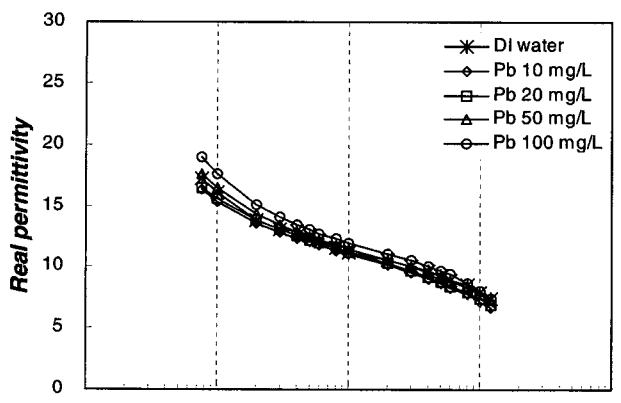
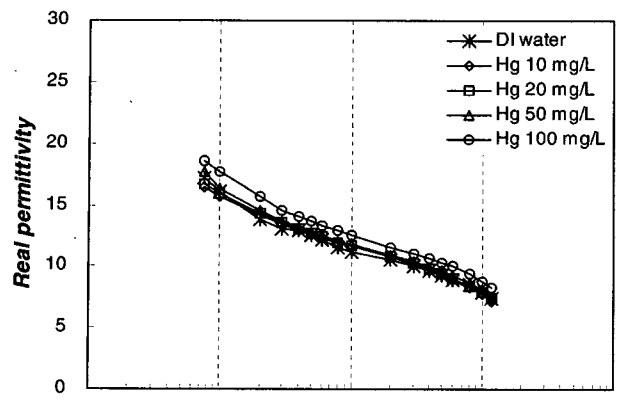
The spectral responses of complex permittivity for mixtures of Jumunjin sand with cationic species aqueous solutions are presented in Figures 5 and 6.

In the case of real permittivity for saturated Jumunjin sand ($\theta_v=0.39$), addition of heavy metal solutions with concentrations above 50 mg/L caused a significant decrease in the real permittivity although the real permittivity showed a little increase in the case of samples with 10 and 20 mg/L concentrations at low frequencies (75 - 500 kHz) (Figure 6 (a)). The drop in real permittivity was observed in Figure 6 (a), for the mixture of the Jumunjin sand with cationic species aqueous solution is in agreement with the trends in real permittivity for the solution itself. However, in the case of real permittivity for Jumunjin sand with lower volumetric water content (Figure 5 (a)), addition of heavy metal caused a little increase of the real permittivity at lower frequencies. The hydration of heavy metals in the soil-heavy metal mixtures leads to reducing the orientation polarization of water molecules

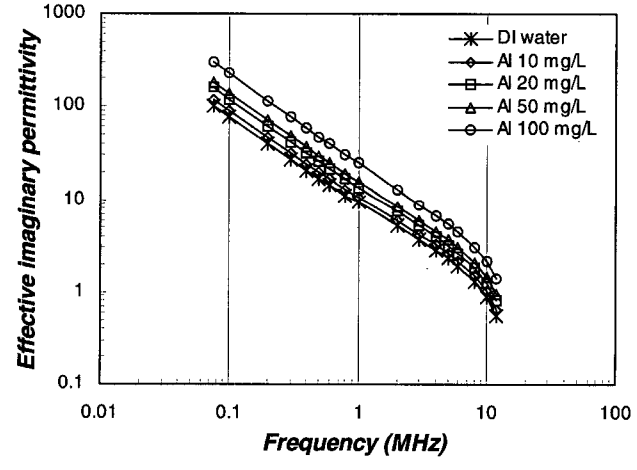
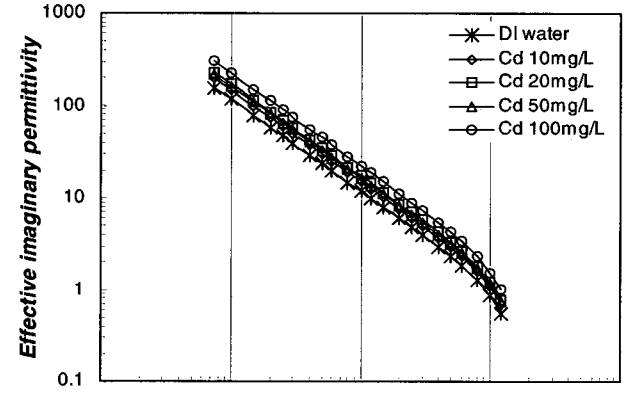
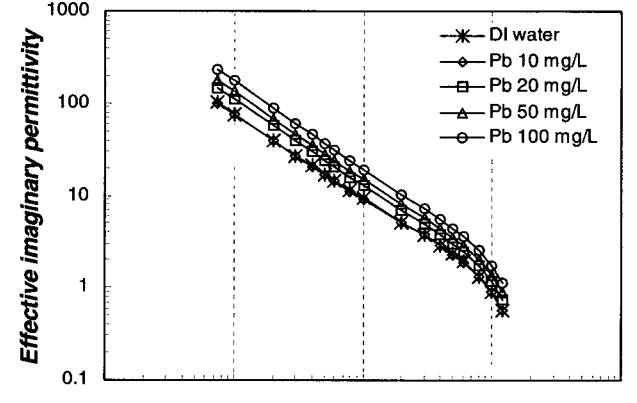
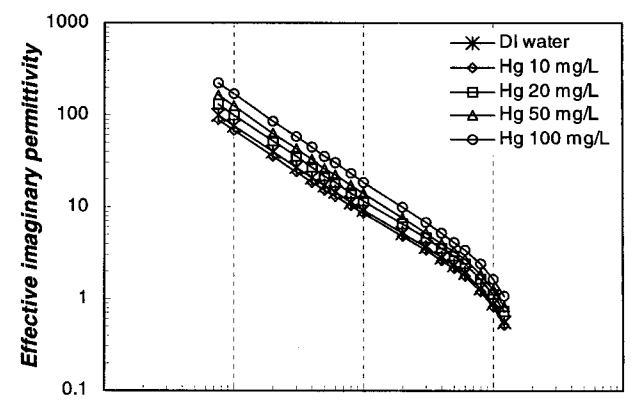
like heavy metal solutions, but spatial polarization of which effect is very large arises in the interface between pore fluid and air or soil particles due to accumulation of ionic constituents at lower frequencies. Therefore, it is interpreted that addition of spatial polarization causes a little increase of real permittivity because the increase in real permittivity from spatial polarization is higher than the decrease from orientation polarization. In this case, spatial polarization increased with concentration since it reflects accumulation of ions at interfaces. However, in saturated Jumunjin sand, water only exists in the pore, hence interface between pore fluid and air disappears. Therefore, the amount of spatial polarization decreases while the reduction of orientation polarization increases due to an increase in heavy metal cations. As a result, the real permittivity of contaminated soil decreases as the concentration of heavy metals increases.

As seen in Figures 5 (b) and 6 (b), the effective imaginary permittivity increased over all frequency ranges studied with increasing cationic concentration of the pore solution. This increase was more significant at higher volumetric water content. Such trends in effective imaginary permittivity reflect improved electrical conductivity of the soil from cationic concentration since effective imaginary permittivity is primarily due to conduction loss.

In order to evaluate whether the complex permittivity was sensitive enough to detect contamination of heavy metals, relative variations defined as the ratio of electrical properties of the contaminated soil to that of uncontaminated soil

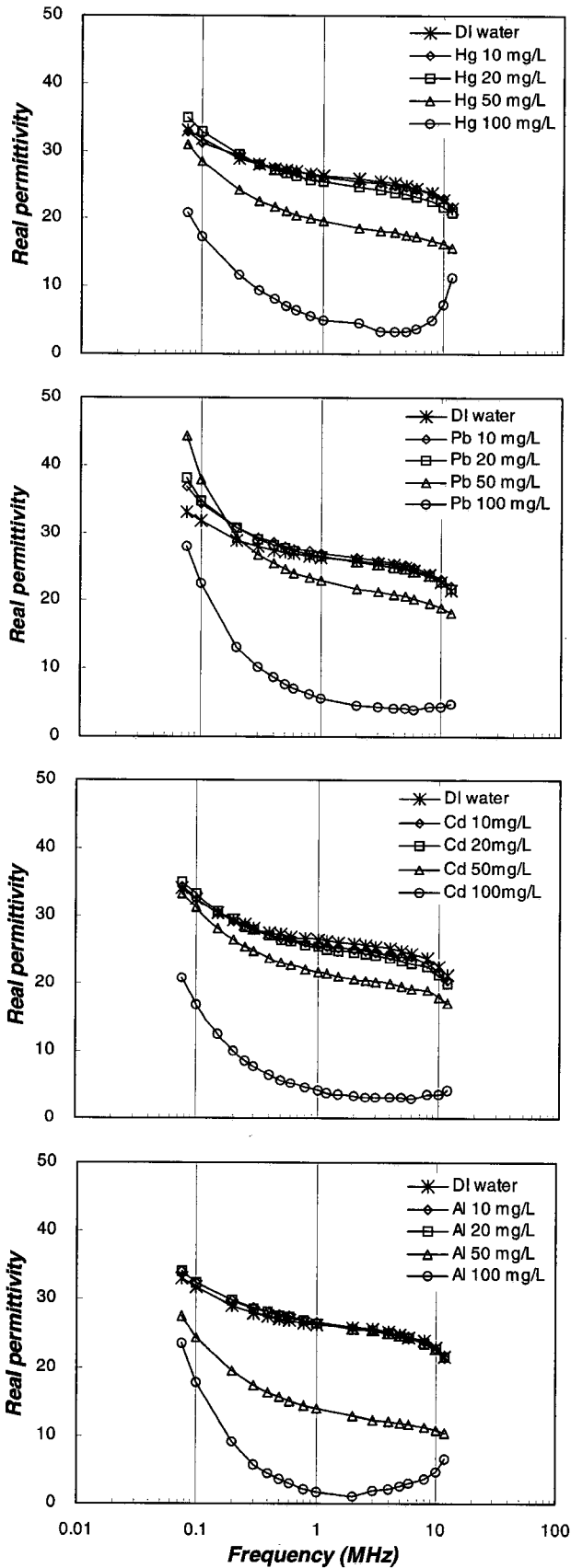


(a) real permittivity

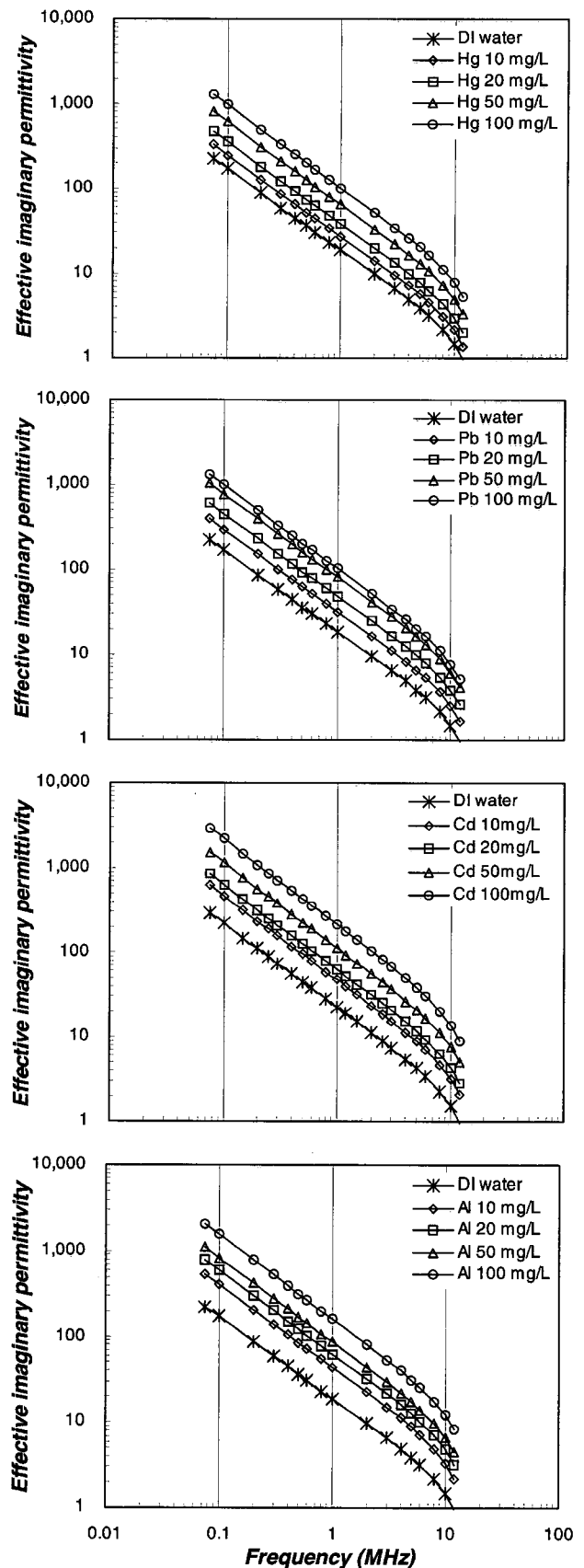


(b) effective imaginary permittivity

Fig. 5. Spectral responses of complex permittivity for mixtures of the Jumunjin sand with cationic species aqueous solution ($\theta_v = 0.13$)



(a) real permittivity



(b) effective imaginary permittivity

Fig. 6. Spectral responses of complex permittivity for mixtures of the Jumunjin sand with cationic species aqueous solution ($\theta_v = 0.39$)

are illustrated for varying concentrations in Figures 7 and 8. The important findings obtained from Figures 7 and 8 are as follows. First, the measurement of real permittivity alone may lead to some degree of ambiguity in the results mainly due to spatial polarization at low volumetric water content. Because the extent of spatial polarization is difficult to quantify, ambiguities in analysis solely on the real permittivities must be overcome. Therefore, an additional measurement and analysis on the effective imaginary permittivity are required in characterizing heavy metal contamination. Secondly, data show that it was difficult to identify ion types using complex permittivity data. Yet, the sensitivity of the effective imaginary permittivity to concentration was found to be valuable in developing electrical methods to detect heavy metals in subsurface. Clear increases in effective imaginary per-

mittivity with concentration were observed although their increment against concentration was small in the case of soils with low volumetric water content. Such changes in electrical properties might be applicable for a detection system using electrical method for contaminant releases into the subsurface. Additionally, the electrical properties of soil are primarily dependent on soil types and volumetric water content. Therefore, in order to utilize the electric measurement method for investigating subsurface contamination, pre-evaluation of soil types and volumetric water content of subsurface is required. Providing the background values based on soil types and volumetric water content, it is highly probable that electrical properties can be used for detecting the contaminant in soils.

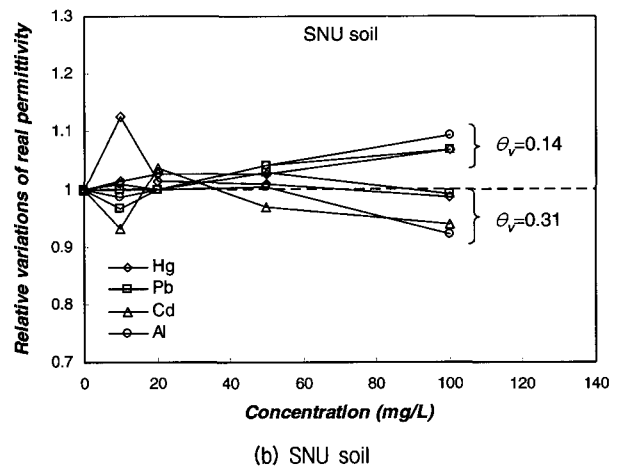
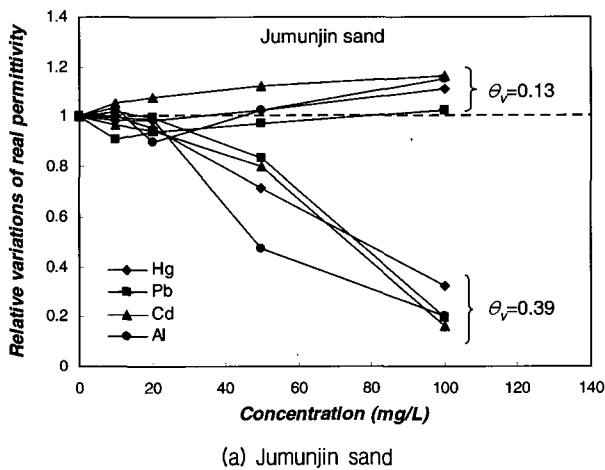


Fig. 7. Relative variations of real permittivity measured at 10 MHz for mixtures of soils with cationic species aqueous solution

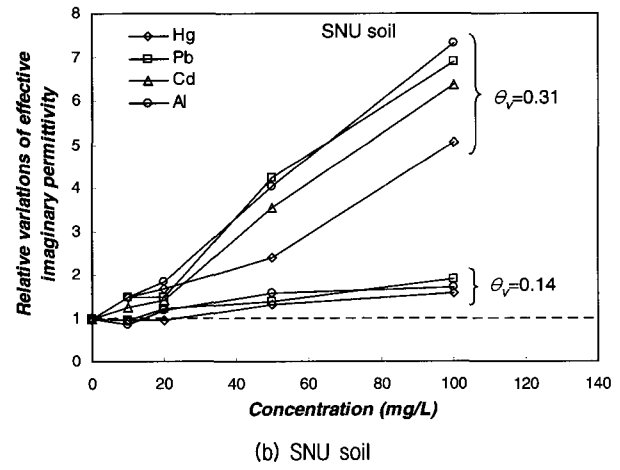
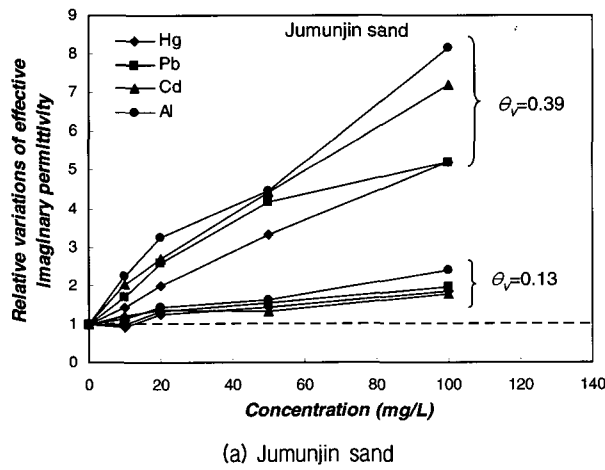


Fig. 8. Relative variations of effective imaginary permittivity measured at 10 MHz for mixtures of soils with cationic species aqueous solution

4. Conclusions

Permittivity of unsaturated sand was strongly governed by the volumetric water content as this is proportional to the number of dipole moments per unit volume. The volumetric water content could be the most effective single parameter for assessing the permittivity of unsaturated soil. A linear relationship between the real permittivity of soil and the volumetric water content was derived at high frequencies (MHz ranges).

Ionic contaminants result in significant increases in the effective imaginary permittivity, due to ionic conduction, but significant decreases in the real permittivity arise due to the decreased orientational polarization of water molecules caused by hydration of ions. However, because the permittivity is primarily dependent on the volumetric water content of soil, pre-evaluation of the volumetric water content is required.

Clear increases in effective imaginary permittivity with concentration of ionic contaminants were observed. Sensitivity of effective imaginary permittivity to concentration is valuable in the application of electrical methods to the detection of heavy metals in the subsurface.

Acknowledgement

This work was supported by grant No. R01-2002-000-00136-0 from the Basic Research Program of the Korea Science & Engineering Foundation.

References

1. ASTM D150 (1994), Standard test methods for AC loss characteristics and permittivity (dielectric constant) of solid electrical insulation, ASTM D150-94, Philadelphia.
2. Darayan, S., Liu, C., Shen, L. C., and Shatthuck, D. (1998), "Measurement of electrical properties of contaminated soil", *Geophysical Prospecting*, 46, pp.477-488.
3. Dean, J. A. (1999), *Lange's Handbook of Chemistry*, 15th Ed. McGraw-Hill, NY.
4. Francisca, F. M. and Rinaldi, V. A. (2003), "Complex dielectric permittivity of soil-organic mixtures (20 MHz - 1.3 GHz)", *Journal of Environmental Engineering*, 129(4), pp.347-357.
5. Fukue, M., Minato, T., Matsumoto, M., Horibe, H., and Taya, N. (2001), "Use of a resistivity cone for detecting contaminated soil layers", *Engineering Geology*, 60, pp.361-369.
6. Gardner, C. M. K., Dean, T. J., and Cooper, J. D. (1998), "Soil water content measurement with a high-frequency capacitance sensor", *Journal of agricultural Engineering Research*, 71, pp. 395-403.
7. Kaya, A and Fang, H. Y. (1997), "Identification of contaminated soils by dielectric constant and electrical conductivity", *Journal of Environmental Engineering*, 123(2), pp.169-177.
8. Lindsay, J. B., Shang, J. Q., and Rowe, R. K. (2002), "Using complex permittivity and artificial neural networks for contaminant prediction", *Journal of Environmental Engineering*, 128(8), pp. 740-747.
9. Lundien, J. R. (1971), "Laboratory measurement of electromagnetic propagation constants in 1.0- to 1.5-GHz microwave special region", Report 5, Terrain Analysis by Electromagnetic Means, Technical Report No.3-693, U.S. Army Engineer Waterways Experiment Station.
10. Oh, M. H., Kim, Y. S., Park, J. B., and Yoon, H. S. (2005), "complex permittivity of sand at low frequency", *Journal of the Korean Geotechnical Society*, Vol.21, No.2, pp.93-103.
11. Okoye, C. N., Cotton, T. R., and O'Meara, D. (1995), "Application of resistivity cone penetration testing for qualitative delineation of creosote contamination in saturated soils", *Proceedings of Geo-environment 2000*, ASCE, New York, pp.151-166.
12. Oxtoby, D. W. and Nachtrieb, N. H. (1996), *Principles of Modern Chemistry*, 3rd Ed., Saunders College Publishing.
13. Rinaldi, V. A. and Cuestas, G. A. (2002), "Ohmic conductivity of a compacted silty clay", *Journal of Geotechnical and Geo-environmental Engineering*, 128(10), pp.824-835.
14. Rinaldi, V. A. and Redolfi, E. R. (1996), "The dielectric constant of soil-NAPL mixtures at low frequencies (100 Hz to 10 MHz)", *Proceeding of Nonaqueous Phase Liquids (NAPLs) in the Subsurface Environment: Assessment and Remediation*, ASCE, Washington D.C., pp.163-174.
15. Robinson, D. A., Gardner, C. M. K., and Cooper, J. D. (1999), "Measurement of relative permittivity in sandy soils using TDR, capacitance and theta probes: comparison, including the effects of bulk soil electrical conductivity", *Journal of Hydrology*, 223, pp.198-211.
16. Rowe, R. K., Shang, J. Q., and Xie, Y. (2001), "Complex permittivity measurement system for detecting soil contamination", *Canadian Geotechnical Journal*, 39, pp.498-506.
17. Rowe, R. K., Shang, J. Q., and Xie, Y. (2002), "Effect of permeating solutions on complex permittivity of compacted clay", *Canadian Geotechnical Journal*, 39, pp.1016-1025.
18. Santamarina, J. C. (2001), *Soils and waves*, John Wiley & Sons.
19. Santamarina, J. C. and Fam, M. (1997), "Dielectric permittivity of soils mixed with organic and inorganic fluids (0.2 GHz to 1.30 GHz)", *Journal of Environmental and Engineering Geophysics*, 2(1), pp.37-51.
20. Thevanayagam, S. (1995), "Frequency-domain analysis of electrical dispersion of soils", *Journal of Geotechnical Engineering*, 121(8), pp.618-628.
21. Topp, G. C., Davis, J. L., and Annan, A. P. (1980), "Electromagnetic determination of soil water content: Measurements in coaxial transmission lines", *Water Resources Research*, 16(3), pp.574-582.
22. Vanysek, P. (2002), "Ionic conductivity and diffusion at finite dilution", In: *CRC Handbook of Chemistry and Physics*, 83rd Ed., CRC Press.
23. Wilson, L. G., Everett, L. G., and Cullen, S. J. (eds.) (1995), *Handbook of Vadose Zone Characterization & Monitoring*, CRC Press.

(received on May 31, 2005, accepted on Jul. 5, 2005)